Nuclear Physics B248 (1984) 29-58
© North-Holland Publishing Company

MESON AND BARYON MASSES FOR LIGHT KOGUT–SUSSKIND QUARKS ON A LARGE LATTICE
(II). Renormalization group analysis

J.P. GILCHRIST and G. SCHIERHOLZ

Deutsches Elektronen-Synchrotron DESY, Hamburg, West Germany

H. SCHNEIDER

Max-Planck-Institut für Physik und Astrophysik, Werner-Heisenberg-Institut für Physik, München, West Germany

M TEPER

LAPP, Annecy, France

Received 15 March 1984

We calculate the low-lying meson and baryon masses in quenched QCD for three different couplings: $\beta = 5.4$, $\beta = 5.7$ and $\beta = 5.9$. The sizes of our lattices are $8^3 \times 16$ ($\beta = 5.4$) and $10^3 \times 16$ ($\beta = 5.7$ and $\beta = 5.9$). We use Kogut–Susskind fermions because they possess an explicit continuous chiral symmetry which we have shown to be broken spontaneously. We find that the meson and baryon masses and the resulting quark mass conform to the continuum renormalization group behaviour to a statistically significant degree. Furthermore, our results are in good agreement with the experimental masses and low-energy parameters for $\Lambda_{\text{mom}} \approx 200$ MeV. This is also roughly the scale parameter one obtains from a variety of other quantities.

1. Introduction

In a recent paper [1] we have presented the first results of a calculation of meson and baryon masses in quenched QCD for light Kogut–Susskind quarks [2] on a large $10^3 \times 16$ lattice. The Kogut–Susskind discretization of the fermion action has the property that it preserves an explicit, continuous chiral symmetry which we have shown [3] to be broken spontaneously. This is prerequisite to a successful description of the low-lying hadron spectrum which is most obviously influenced by the dynamics of chiral symmetry and its spontaneous breakdown.

The widely used Wilson fermion action [4] explicitly breaks all chiral symmetries by operators which will become irrelevant deep in the continuum limit. In the region of couplings accessible to Monte Carlo calculations at present there is, however, no evidence that the Wilson action has recovered chiral symmetry enough to break it spontaneously. (A recent investigation [5] which addresses this question in SU(2) suggests that continuum chiral symmetry and its subsequent spontaneous breaking is indeed not yet realized.) This disfavours the Wilson discretization of the fermion action for spectrum calculations. In particular the standard procedure (for the

present state of the art see [6]) of extrapolating the mass measurements taken at large "pion" mass to zero "pion" mass to obtain the bound states of light quarks must be questioned in a theory that (perhaps) has not yet developed a Goldstone pion.

To be sensitive to the physics of spontaneous chiral symmetry breaking, we have emphasized [1] that we must choose the invariant quark mass to be $m_q \ll \Lambda_{mom}$. This criterion is not fulfilled by any of the previous calculations [7, 8]. Due to convergence problems with the Gauss–Seidel and hopping parameter exapansions they were made for quark masses of hundreds of MeV, and then the light quark physics is obtained by means of extrapolations of unknown reliability. We have calculated with invariant quark masses in the range 10 to 80 MeV using the conjugate gradient algorithm and find very accurate convergence.

So far our calculation [1] of meson and baryon masses was done at the single value of $\beta = 5.7$. We found that the experimental low-lying hadron masses and low-energy parameters are well reproduced for $\Lambda_{mom} \approx 200$ MeV. This is also roughly the scale parameter one obtains from a variety of other quantities [9] – in contrast to Monte Carlo calculations [8] using Wilson fermions. (For a more detailed comparison of Λ parameters see the end of this paper.) For this Λ_{mom} the $10^3 \times 16$ lattice has the physical volume of $(2.8\,\text{fm})^3$ which (for antiperiodic boundary conditions) we found to be large enough to accommodate the dynamics of light quarks [1, 3]. In the meantime our results for the meson and baryon masses have been confirmed by the Edinburgh group [10].

To show that the masses we have calculated are those of the continuum theory, we must redo the calculation over a range of β values and demonstrate the correct renormalization group behaviour. In this paper we repeat our calculation at $\beta = 5.4$ and $\beta = 5.9$. Between these two values the lattice spacing varies by a factor of ≈ 1.75 which should reveal any significant nonadherence to the desired continuum behaviour.

The paper is organized as follows. In sect. 2 we present meson and baryon propagators for Kogut–Susskind staggered fermions that are of interest to us here. In sect. 3 we discuss the essentials of our calculation and present the results for the correlation functions. The procedure of extracting the meson and baryon masses is also described. The masses and further results are presented in sect. 4. We conclude with some remarks in sect. 5.

2. Meson and baryon propagators

We assume that the reader is familiar with the notation of Kogut–Susskind staggered fermions [2, 11]. In this paper we shall study only those flavours of mesons and baryons that can be constructed out of operators which are local on the original lattice. These are [11] for the mesons

$$J_\lambda(z) = \sum_A \bar{q}_A(z)(\Gamma_\lambda \otimes \Gamma_\lambda^*) q_A(z)\,, \tag{1}$$

and for the baryons

$$\Psi^{\mu f}(z) = \sum_{\substack{\eta \\ A,B,C \\ \mu',f'}} \varepsilon_{ABC} \Gamma_\eta^{\mu\mu'} \Gamma_\eta^{*ff'} q_A^{\mu' f'}(z) [q_B(z)(\mathbb{C}\Gamma_\eta \otimes \mathbb{C}^* \Gamma_\eta^*) q_C(z)] , \tag{2}$$

where μ labels the Dirac component and f, A label flavour and colour, respectively. In eqs. (1), (2) the quark fields are given by

$$q_A^{\mu f}(z) = \sum_\eta \Gamma_\eta^{\mu f} U_\eta^{AA'}(z) \chi_{A'}(2z+\eta) , \tag{3}$$

where $U_\eta^{AA'}(z)$ is the product of link variables over a definite path going from $2z$ to $2z+\eta$. The sum over η runs over the 2^4 sites of the hypercube labelled by z, and the 16 matrices Γ_η associated with them form a basis of the Cifford algebra generated by the Dirac matrices γ_μ. The single-component fermionic fields χ in eq. (3) (which act on the original lattice) are coupled by the action [1]

$$S_F = - \sum_{\substack{z,\eta,\eta' \\ A,A'}} \bar{\chi}_A(2z+\eta) [\mathcal{M}(U)^{AA'}_{2z+\eta,2z+\eta'} + 2ma\delta^{AA'}\delta_{\eta\eta'}] \chi_{A'}(2z+\eta') . \tag{4}$$

In terms of these fields the mesonic and baryonic operators (1), (2) read

$$J_\lambda(z) = \sum_{\substack{\eta \\ A}} \mathrm{Tr}\,(\Gamma_\eta^+ \Gamma_\lambda \Gamma_\eta \Gamma_\lambda^+) \bar{\chi}_A(2z+\eta) \chi_A(2z+\eta) , \tag{5}$$

$$\Psi^{\mu f}(z) = \sum_{\substack{\eta \\ A,B,C}} \varepsilon_{ABC} \Gamma_\eta^{\mu f} \chi_A(2z+\eta) \chi_B(2z+\eta) \chi_C(2z+\eta) . \tag{6}$$

We shall deal with nonlocal operators and the question of restoration of isospin invariance in a separate publication.

The meson and baryon masses will be obtained from the exponential decay in time of the correlation functions of the mesonic and baryonic operators (1), (2). In this section we shall investigate these correlation functions in a little more detail than was possible in the letter [1].

2.1. MESONS

For the mesons we consider the operators (1) being given by the following set of Γ_λ's:

Γ_λ	flavour
$\left.\begin{matrix}\gamma_5 \\ \gamma_0\gamma_5\end{matrix}\right\}$	π
$\left.\begin{matrix}\boldsymbol{\gamma} \\ \gamma_0\boldsymbol{\gamma}\end{matrix}\right\}$	ρ
$\gamma_5\boldsymbol{\gamma}$	A_1
$\frac{1}{2}\boldsymbol{\gamma}\times\boldsymbol{\gamma}$	B
1	ε .

(7)

The associated flavour quantum numbers are indicated in the second column by the lowest-lying meson in the corresponding channel. The meson called the ε is the iso-singlet scalar state which is not to be confused with the S^* or δ. All other states spanned by the local operators (1) are non-singlet states. The operators (7) exhaust all possible different local correlation functions. They lead to

$$\begin{aligned} M_{\gamma_5}(t) &= \sum_z \sum_{A,B} \langle \bar{q}_A(z,t)(\gamma_5 \otimes \gamma_5) q_A(z,t) \bar{q}_B(0)(\gamma_5 \otimes \gamma_5) q_B(0)\rangle \\ &= 32 \sum_x \sum_{A,B} [2\langle |\bar{\chi}_A(x,2t)\chi_B(0)|^2\rangle \\ &\quad + \langle |\bar{\chi}_A(x,2t+1)\chi_B(0)|^2\rangle + \langle |\bar{\chi}_A(x,2t-1)\chi_B(0)|^2\rangle], \end{aligned} \tag{8}$$

$$\begin{aligned} M_{\gamma_0\gamma_5}(t) &= \sum_z \sum_{A,B} \langle \bar{q}_A(z,t)(\gamma_0\gamma_5 \otimes \gamma_0\gamma_5) q_A(z,t) \bar{q}_B(0)(\gamma_0\gamma_5 \otimes \gamma_0\gamma_5) q_B(0)\rangle \\ &= 32 \sum_x \sum_{A,B} (-1)^{\hat{x}_1+\hat{x}_2+\hat{x}_3}[2\langle |\bar{\chi}_A(x,2t)\chi_B(0)|^2\rangle \\ &\quad + \langle |\bar{\chi}_A(x,2t+1)\chi_B(0)|^2\rangle + \langle |\bar{\chi}_A(x,2t-1)\chi_B(0)|^2\rangle], \end{aligned} \tag{9}$$

$$\begin{aligned} M_{\gamma}(t) &= \sum_z \sum_{A,B} \sum_{i=1}^{3} \langle \bar{q}_A(z,t)(\gamma_i \otimes \gamma_i) q_A(z,t) \bar{q}_B(0)(\gamma_i \otimes \gamma_i) q_B(0)\rangle \\ &= 32 \sum_x \sum_{A,B} [(-1)^{\hat{x}_1} + (-1)^{\hat{x}_2} + (-1)^{\hat{x}_3}][2\langle |\bar{\chi}_A(x,2t)\chi_B(0)|\rangle \\ &\quad + \langle |\bar{\chi}_A(x,2t+1)\chi_B(0)|^2\rangle + \langle |\bar{\chi}_A(x,2t-1)\chi_B(0)|^2\rangle], \end{aligned} \tag{10}$$

$$\begin{aligned} M_{\gamma_0\gamma}(t) &= \sum_z \sum_{A,B} \sum_{i=1}^{3} \langle \bar{q}_A(z,t)(\gamma_0\gamma_i \otimes \gamma_0\gamma_i) q_A(z,t) \bar{q}_B(0)(\gamma_0\gamma_i \otimes \gamma_0\gamma_i) q_B(0)\rangle \\ &= 32 \sum_x \sum_{A,B} [(-1)^{\hat{x}_2+\hat{x}_2} + (-1)^{\hat{x}_1+\hat{x}_3} + (-1)^{\hat{x}_1+\hat{x}_2}][2\langle |\bar{\chi}_A(x,2t)\chi_B(0)|^2\rangle \\ &\quad + \langle |\bar{\chi}_A(x,2t+1)\chi_B(0)|^2\rangle + \langle |\bar{\chi}_A(x,2t-1)\chi_B(0)|^2\rangle], \end{aligned} \tag{11}$$

$$\begin{aligned} M_{\gamma_5\gamma}(t) &= \sum_z \sum_{A,B} \sum_{i=1}^{3} \langle \bar{q}_A(z,t)(\gamma_5\gamma_i \otimes \gamma_5\gamma_i) q_A(z,t) \bar{q}_B(0)(\gamma_5\gamma_i \otimes \gamma_5\gamma_i) q_B(0)\rangle \\ &= 32 \sum_x \sum_{A,B} [(-1)^{\hat{x}_2+\hat{x}_3} + (-1)^{\hat{x}_1+\hat{x}_3} + (-1)^{\hat{x}_1+\hat{x}_2}][2\langle |\bar{\chi}_A(x,2t)\chi_B(0)|^2\rangle \\ &\quad - \langle |\bar{\chi}_A(x,2t+1)\chi_B(0)|^2\rangle - \langle |\bar{\chi}_A(x,2t-1)\chi_B(0)|^2\rangle], \end{aligned} \tag{12}$$

$$\begin{aligned} M_{\gamma\times\gamma}(t) &= \sum_z \sum_{A,B} \sum_{\substack{i,j=1 \\ i<j}}^{3} \langle \bar{q}_A(z,t)(\gamma_i\gamma_j \otimes \gamma_i\gamma_j) q_A(z,t) \bar{q}_B(0)(\gamma_i\gamma_j \otimes \gamma_i\gamma_j) q_B(0)\rangle \\ &= 32 \sum_x \sum_{A,B} [(-1)^{\hat{x}_1} + (-1)^{\hat{x}_2} + (-1)^{\hat{x}_3}][2\langle |\bar{\chi}_A(x,2t)\chi_B(0)|^2\rangle \\ &\quad - \langle |\bar{\chi}_A(x,2t+1)\chi_B(0)|^2\rangle - \langle |\bar{\chi}_A(x,2t-1)\chi_B(0)|^2\rangle], \end{aligned} \tag{13}$$

$$M_1(t) = \sum_z \sum_{A,B} \langle \bar{q}_A(z,t)(1\otimes 1)q_A(z,t)\bar{q}_B(0)(1\otimes 1)q_B(0)\rangle$$
$$= 32\sum_x \sum_{A,B} (-1)^{\hat{x}_1+\hat{x}_2+\hat{x}_3}[2\langle|\bar{\chi}_A(x,2t)\chi_B(0)|^2\rangle$$
$$-\langle|\bar{\chi}_A(x,2t+1)\chi_B(0)|^2\rangle - \langle|\bar{\chi}_A(x,2t-1)\chi_B(0)|^2\rangle], \tag{14}$$

where $x = (\hat{x}_1, \hat{x}_2, \hat{x})a$ runs over the original lattice. At large t the correlation functions (8)–(14) receive contributions from only a few low-lying states:

$$M_{\gamma_5}(t) = K_\pi(e^{-m_\pi 2t} + e^{-m_\pi(T-2t)}) + \cdots,$$
$$M_{\gamma_0\gamma_5}(t) = K'_\pi(e^{-m_\pi 2t} + e^{-m_\pi(T-2t)}) + \cdots,$$
$$M_\gamma(t) = K_\rho(e^{-m_\rho 2t} + e^{-m_\rho(T-2t)}) + \cdots,$$
$$M_{\gamma_0\gamma}(t) = K'_\rho(e^{-m_\rho 2t} + e^{-m_\rho(T-2t)}) + \cdots,$$
$$M_{\gamma_5\gamma}(t) = K_{A_1}(e^{-m_{A_1} 2t} + e^{-m_{A_1}(T-2t)}) + \cdots,$$
$$M_{\gamma\times\gamma}(t) = K_B(e^{-m_B 2t} + e^{-m_B(T-2t)}) + \cdots,$$
$$M_1(t) = K_\varepsilon(e^{-m_\varepsilon 2t} + e^{-m_\varepsilon(T-2t)}) + \cdots, \tag{15}$$

where T is the temporal extent of the lattice. Throughout this paper we shall use antiperiodic fermionic boundary conditions.

The correlation functions introduced earlier on [1, 12] ($t = \hat{t}a$):

$$M_{PS}(t) = \sum_x \sum_{A,B} \langle|\bar{\chi}_A(x,t)\chi_B(0)|^2\rangle,$$
$$M_{V-T}(t) = \sum_x \sum_{A,B} [(-1)^{\hat{x}_1} + (-1)^{\hat{x}_2} + (-1)^{\hat{x}_3}]\langle|\bar{\chi}_A(x,t)\chi_B(0)|^2\rangle,$$
$$M_{PV}(t) = \sum_x \sum_{A,B} [(-1)^{\hat{x}_2+\hat{x}_3} + (-1)^{\hat{x}_1+\hat{x}_3} + (-1)^{\hat{x}_1+\hat{x}_2}]\langle|\bar{\chi}_A(x,t)\chi_B(0)|^2\rangle,$$
$$M_S(t) = \sum_x \sum_{A,B} (-1)^{\hat{x}_1+\hat{x}_2+\hat{x}_3+\hat{t}}\langle|\chi_A(x,t)\chi_B(0)|^2\rangle, \tag{16}$$

which extend over even *and* odd $\hat{t}$, have twice as many entries as the correlation functions (8)–(15) and are therefore preferred for Monte Carlo calculations. They are related to (8)–(15) by

$$M_{\gamma_5}(t) = 32[2M_{PS}(2t) + M_{PS}(2t+1) + M_{PS}(2t-1)],$$
$$M_{\gamma_0\gamma_5}(t) = 32[2M_S(2t) - M_S(2t+1) - M_S(2t-1)],$$
$$M_\gamma(t) = 32[2M_{V-T}(2t) + M_{V-T}(2t+1) + M_{V-T}(2t-1)],$$
$$M_{\gamma_0\gamma}(t) = 32[2M_{PV}(2t) - M_{PV}(2t+1) - M_{PV}(2t-1)],$$
$$M_{\gamma_5\gamma}(t) = 32[2M_{PV}(2t) + M_{PV}(2t+1) + M_{PV}(2t-1)],$$

$$M_{\gamma\times\gamma}(t)=32[2M_{\mathrm{V-T}}(2t)-M_{\mathrm{V-T}}(2t+1)-M_{\mathrm{V-T}}(2t-1)],$$
$$M_{\mathrm{I}}(t)=32[2M_{\mathrm{S}}(2t)+M_{\mathrm{S}}(2t+1)+M_{\mathrm{S}}(2t-1)]. \tag{17}$$

We may solve this set of equations for $M_{\mathrm{PS}}(t)$, $M_{\mathrm{V-T}}(t)$, $M_{\mathrm{PV}}(t)$, $M_{\mathrm{S}}(t)$ by making use of the explicit form (15) of the correlation functions (8)–(15). We obtain

$$M_{\mathrm{PS}}(t)=\frac{1}{32}\frac{1}{2(1+\cosh(m_\pi a))}K_\pi(\mathrm{e}^{-m_\pi t}+\mathrm{e}^{-m_\pi(T-t)})+\cdots,$$

$$\begin{aligned}M_{\mathrm{V-T}}(t)=\frac{1}{32}\Bigg\{&\frac{1+\cosh(m_\rho a)}{8\cosh(m_\rho a)}K_\rho(\mathrm{e}^{-m_\rho t}+\mathrm{e}^{-m_\rho(T-t)}\\&-\frac{1-\cosh(m_{\mathrm{B}}a)}{8\cosh(m_{\mathrm{B}}a)}K_{\mathrm{B}}(\mathrm{e}^{-m_{\mathrm{B}}t}+\mathrm{e}^{-m_{\mathrm{B}}(T-t)})\\&+(-1)^{\hat{t}}\Bigg[\frac{1+\cosh(m_{\mathrm{B}}a)}{8\cosh(m_{\mathrm{B}}a)}K_{\mathrm{B}}(\mathrm{e}^{-m_{\mathrm{B}}t}+\mathrm{e}^{-m_{\mathrm{B}}(T-t)})\\&-\frac{1-\cosh(m_\rho a)}{8\cosh(m_\rho a)}K_\rho(\mathrm{e}^{-m_\rho t}+\mathrm{e}^{-m_\rho(T-t)})\Bigg]\Bigg\}+\cdots,\end{aligned}$$

$$\begin{aligned}M_{\mathrm{PV}}(t)=\frac{1}{32}\Bigg\{&\frac{1+\cosh(m_{\mathrm{A_1}}a)}{8\cosh(m_{\mathrm{A_1}}a)}K_{\mathrm{A_1}}(\mathrm{e}^{-m_{\mathrm{A_1}}t}+\mathrm{e}^{-m_{\mathrm{A_1}}(T-t)})\\&-\frac{1-\cosh(m_\rho a)}{8\cosh(m_\rho a)}K'_\rho(\mathrm{e}^{-m_\rho t}+\mathrm{e}^{-m_\rho(T-t)})\\&+(-1)^{\hat{t}}\Bigg[\frac{1+\cosh(m_\rho a)}{8\cosh(m_\rho a)}K'_\rho(\mathrm{e}^{-m_\rho t}+\mathrm{e}^{-m_\rho(T-t)})\\&-\frac{1-\cosh(m_{\mathrm{A_1}}a)}{8\cosh(m_{\mathrm{A_1}}a)}K_{\mathrm{A_1}}(\mathrm{e}^{-m_{\mathrm{A_1}}t}+\mathrm{e}^{-m_{\mathrm{A_1}}(T-t)})\Bigg]\Bigg\}+\cdots,\end{aligned}$$

$$\begin{aligned}M_{\mathrm{S}}(t)=\frac{1}{32}\Bigg\{&\frac{1+\cosh(m_\varepsilon a)}{8\cosh(m_\varepsilon a)}K_\varepsilon(\mathrm{e}^{-m_\varepsilon t}+\mathrm{e}^{-m_\varepsilon(T-t)})\\&-\frac{1-\cosh(m_\pi a)}{8\cosh(m_\pi a)}K'_\pi(\mathrm{e}^{-m_\pi t}+\mathrm{e}^{-m_\pi(T-t)})\\&+(-1)^{\hat{t}}\Bigg[\frac{1+\cosh(m_\pi a)}{8\cosh(m_\pi a)}K'_\pi(\mathrm{e}^{-m_\pi t}+\mathrm{e}^{-m_\pi(T-t)})\\&-\frac{1-\cosh(m_\varepsilon a)}{8\cosh(m_\varepsilon a)}K_\varepsilon(\mathrm{e}^{-m_\varepsilon t}+\mathrm{e}^{-m_\varepsilon(T-t)})\Bigg]\Bigg\}+\cdots.\end{aligned} \tag{18}$$

These are the correct expressions of (16) in terms of the physical masses. For $m_\pi a$, $m_\rho a$, $m_{\mathrm{B}}a$, $m_{\mathrm{A_1}}a$, $m_\varepsilon a\to 0$ they go over into the parametrizations given earlier on in refs. [1] (eq. (11)) and [7] with $K_{\pi,\rho,\ldots}=128C_{\pi,\rho,\ldots}$.

2.2 BARYONS

The baryonic operator (2) transforms like a spin-$\frac{1}{2}$ operator on the lattice. Baryonic states of definite parity, ± 1, correspond to the operators

$$\Psi_{\pm}^{\mu f}(z, t) = \left(\frac{1 \pm \gamma_0}{2}\right)^{\mu\mu'} \Psi^{\mu' f}(-z, t) . \tag{19}$$

They lead to the correlation functions

$$\begin{aligned} B_{\pm}(t) &= \sum_{z} \sum_{\mu, f} \langle \Psi_{\pm}^{\mu f}(z, t) \Psi_{\pm}^{\mu f}(0) \rangle \\ &= 32 \sum_{z} \sum_{\substack{A,B,C \\ A',B',C'}} \varepsilon_{ABC} \varepsilon_{A'B'C'} [2 \langle \bar{\chi}_A(2z, 2t) \bar{\chi}_B(2z, 2t) \bar{\chi}_C(2z, 2t) \chi_{A'}(0) \chi_{B'}(0) \chi_{C'}(0) \rangle \\ &\quad \pm \langle \bar{\chi}_A(2z, 2t+1) \bar{\chi}_B(2z, 2t+1) \bar{\chi}_C(2z, 2t+1) \chi_{A'}(0) \chi_{B'}(0) \chi_{C'}(0) \rangle \\ &\quad \pm \langle \bar{\chi}_A(2z, 2t-1) \bar{\chi}_B(2z, 2t-1) \bar{\chi}_C(2z, 2t-1) \chi_{A'}(0) \chi_{B'}(0) \chi_{C'}(0) \rangle] . \end{aligned} \tag{20}$$

Note that the sum over the spacial lattice runs only over even lattice points. For large t this can be written (for antiperiodic fermionic boundary conditions)

$$\begin{aligned} B_{+}(t) &= K_{\mathrm{N}} \, \mathrm{e}^{-m_{\mathrm{N}} 2t} + K_{\mathrm{N}'} \, \mathrm{e}^{-m_{\mathrm{N}'} 2t} + K_{\mathrm{N}^-} \, \mathrm{e}^{-m_{\mathrm{N}^-}(T-2t)} + \cdots , \\ B_{-}(t) &= -K_{\mathrm{N}^-} \, \mathrm{e}^{-m_{\mathrm{N}^-} 2t} - K_{\mathrm{N}} \, \mathrm{e}^{-m_{\mathrm{N}}(T-2t)} - K_{\mathrm{N}'} \, \mathrm{e}^{-m_{\mathrm{N}'}(T-2t)} + \cdots , \end{aligned} \tag{21}$$

where m_{N} is the nucleon mass, $m_{\mathrm{N}'}$ that of the first excited $J^P = \frac{1}{2}^+$ state and m_{N^-} is the mass of the lowest $J^P = \frac{1}{2}^-$ state.

In terms of the originally introduced correlation function [1]

$$B(t) = \sum_{x_1, x_2, x_3 = \text{even}} \sum_{\substack{A,B,C \\ A',B',C'}} \varepsilon_{ABC} \varepsilon_{A'B'C'} \langle \bar{\chi}_A(x, t) \bar{\chi}_B(x, t) \bar{\chi}_C(x, t) \chi_{A'}(0) \chi_{B'}(0) \chi_{C'}(0) \rangle , \tag{22}$$

eq. (20) reads

$$B_{\pm}(t) = 32[2B(2t) \pm B(2t+1) \pm B(2t-1)] . \tag{23}$$

This may be solved for $B(t)$ using (21). We find

$$\begin{aligned} B(t) = \frac{1}{32} \Bigg\{ & \frac{1 + \cosh(m_{\mathrm{N}} a)}{8 \cosh(m_{\mathrm{N}} a)} K_{\mathrm{N}} (\mathrm{e}^{-m_{\mathrm{N}} t} - (-1)^{\hat{t}} \, \mathrm{e}^{-m_{\mathrm{N}}(T-t)}) \\ & + \frac{1 + \cosh(m_{\mathrm{N}'} a)}{8 \cosh(m_{\mathrm{N}'} a)} K_{\mathrm{N}'} (\mathrm{e}^{-m_{\mathrm{N}'} t} - (-1)^{\hat{t}} \, \mathrm{e}^{-m_{\mathrm{N}'}(T-t)}) \\ & + \frac{1 - \cosh(m_{\mathrm{N}^-} a)}{8 \cosh(m_{\mathrm{N}^-} a)} K_{\mathrm{N}^-} (\mathrm{e}^{-m_{\mathrm{N}^-} t} - (-1)^{\hat{t}} \, \mathrm{e}^{-m_{\mathrm{N}^-}(T-t)}) \\ & - (-1)^{\hat{t}} \Bigg[\frac{1 + \cosh(m_{\mathrm{N}^-} a)}{8 \cosh(m_{\mathrm{N}^-} a)} K_{\mathrm{N}^-} (\mathrm{e}^{-m_{\mathrm{N}^-} t} - (-1)^{\hat{t}} \, \mathrm{e}^{-m_{\mathrm{N}^-}(T-t)}) \end{aligned}$$

$$+\frac{1-\cosh(m_{\mathrm{N}}a)}{8\cosh(m_{\mathrm{N}}a)}K_{\mathrm{N}}(\mathrm{e}^{-m_{\mathrm{N}}t}-(-1)^{\hat{t}}\,\mathrm{e}^{-m_{\mathrm{N}}(T-t)})$$

$$+\frac{1-\cosh(m_{\mathrm{N}'}a)}{8\cosh(m_{\mathrm{N}'}a)}K_{\mathrm{N}'}(\mathrm{e}^{-m_{\mathrm{N}'}t}-(-1)^{\hat{t}}\,\mathrm{e}^{-m_{\mathrm{N}'}(T-t)})\Bigg]\Bigg\}+\cdots. \tag{24}$$

For $m_{\mathrm{N}}a$, $m_{\mathrm{N}'}a$, $m_{\mathrm{N}^-}a\to 0$ (24) reduces to the form given in ref. [1] with $K_{\mathrm{N},\ldots}=128C_{\mathrm{N},\ldots}$, $K_{\mathrm{N}^-,\ldots}=-128C_{\mathrm{N}^-,\ldots}$.

The correlation functions (16), (22) and their parameterizations (18), (24) will form the basis of our calculation of meson and baryon masses to be discussed in the next sections.

3. Calculation of quark propagators and correlation functions

We follow the same procedure as in ref. [1] to calculate the quark propagators

$$\bar{\chi}_A(x,t)\chi_B(0)=[(\mathcal{M}(U)+2ma)^{-1}]^{AB}_{(x,t),0}, \tag{25}$$

for any given background gauge field configuration. The size of our lattice is $8^3\times 16$ at $\beta=5.4$ and $10^3\times 16$ at $\beta=5.7$ and $\beta=5.9$. At $\beta=5.4$ we have calculated a total of 96 quark propagators ($\times 3$ colours) on 6 independent gauge field configurations, at $\beta=5.7$ we have computed 112 propagators on 7 configurations and at $\beta=5.9$ we have calculated 104 quark propagators on 13 independent gauge field configurations. The origin $(x,t)=0$ is chosen so that the quark starts well away from the spatial boundaries and that the propagators calculated on the same background gauge field configuration are as independent as they can be. All calculations are done at 3 different quark masses: $ma=0.015$, $ma=0.04$, $ma=0.07$ at $\beta=5.4$ and $ma=0.01$, $ma=0.03$, $ma=0.05$ at $\beta=5.7$ and $\beta=5.9$.

3.1. $\langle\bar{\psi}\psi\rangle$

Our calculation of quark propagators gives, as a by-product, the chiral condensate [3]

$$\langle\bar{\psi}\psi(m)\rangle=\sum_A\langle\bar{\chi}_A(0)\chi_A(0)\rangle=\frac{3}{N}\langle\mathrm{Tr}\,(\mathcal{M}+2ma)^{-1}\rangle \tag{26}$$

(where $N=3L_{\mathrm{s}}^3\times L_{\mathrm{t}}$, $L_{\mathrm{s}}(L_{\mathrm{t}})$ being the spatial (temporal) size of the lattice). To compare $\langle\bar{\psi}\psi\rangle$ with our earlier results [3] obtained on the 8^4 lattice (using the Lanczos algorithm) and to check for finite volume dependences, we have plotted $\langle\bar{\psi}\psi(m)\rangle$ for the masses we consider here in fig. 1 together with our previous values. We observe no difference. This is to say that the $8^3\times 16$ lattice at $\beta=5.4$ and the $10^3\times 16$ lattice at $\beta\leqslant 5.9$ is, for the quark masses considered, essentially of infinite volume as far as the the dynamics of spontaneous chiral symmetry breaking is concerned.

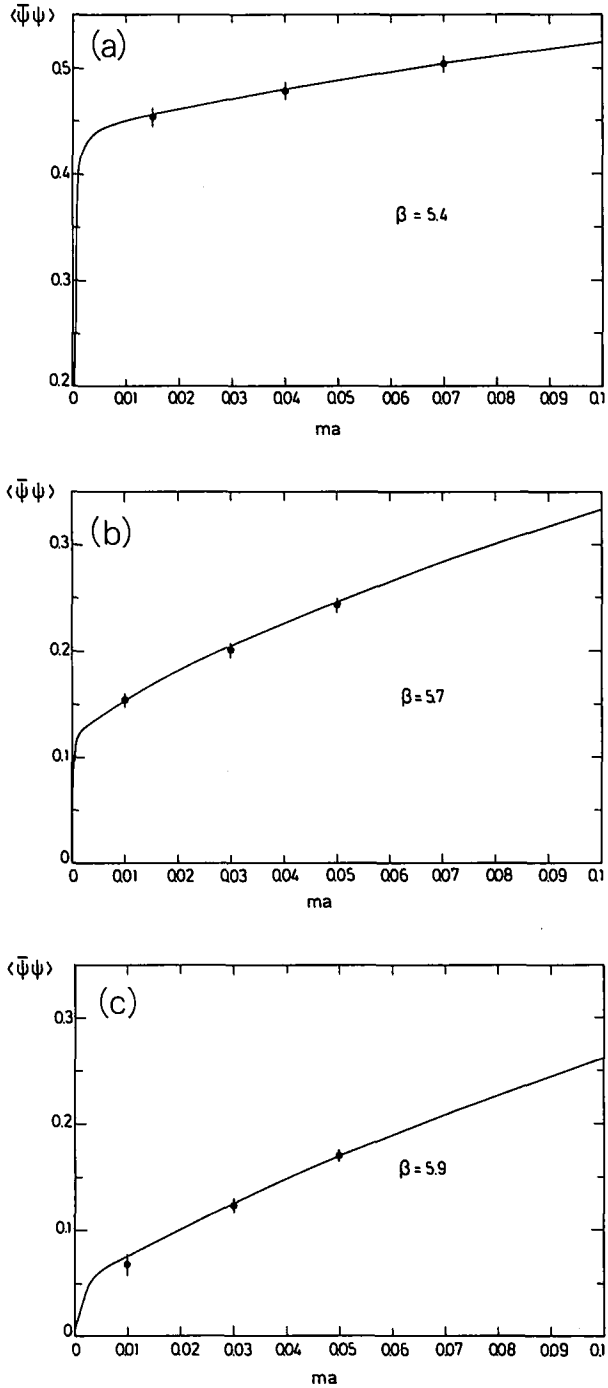

Fig. 1. $\langle\bar{\psi}\psi\rangle$ as a function of the bare mass for (a) $\beta = 5.4$, (b) $\beta = 5.7$ and (c) $\beta = 5.9$. The solid lines are from ref. [3] on the 8^4 lattice. The solid circles are from the spectrum calculations in this work.

3.2. CORRELATION FUNCTIONS

We obtain the correlation functions (16), (22) by multiplying together the individual quark propagators in the appropriate fashion and then averaging over the whole lot. To reproduce the exponential decay of the meson and baryon propagators over several orders of magnitude, we have to calculate the quark propagators to a high accuracy. We monitor the values of [1] r_i^2 during the calculation and stop the iterative procedures once $r_i^2 \leq 10^{-8}$. This, we have checked, guarantees an accuracy of the smallest elements of the quark propagators (i.e. the large-distance piece) of better than one per cent.

In figs. 2–13 we show a selection of correlation functions we obtain at $\beta = 5.4$, $\beta = 5.7$ and $\beta = 5.9$. M_{PS} (figs. 2, 6, 10a, b), which contains the π and hence gives the largest signal, stands out by having very small errors (of the size of the solid circles or smaller) all the way down to $\hat{t} = 8$. The correlation function M_{V-T} (figs. 3, 7, 11a, b), being a combination of ρ, B, etc. propagators, shows an oscillating behaviour (the solid circles) over even and odd $\hat{t}$ as we expect. The same is also found for M_{PV} which we have not plotted here for reasons of space. The amplitude of oscillation increases with increasing β (decreasing a) which favours the larger

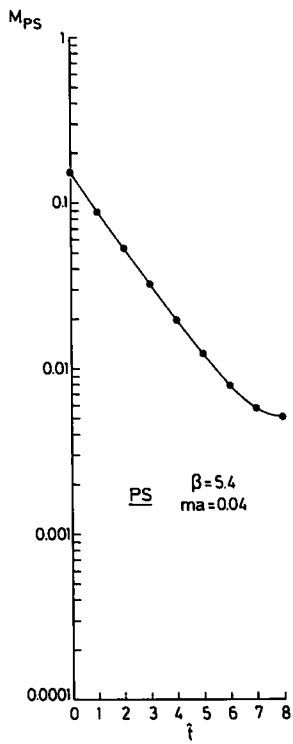

Fig. 2. The correlation functions M_{PS} for $\beta = 5.4$ and $ma = 0.04$. The solid circles are the results of our calculation. The solid line is the fit as described in the text.

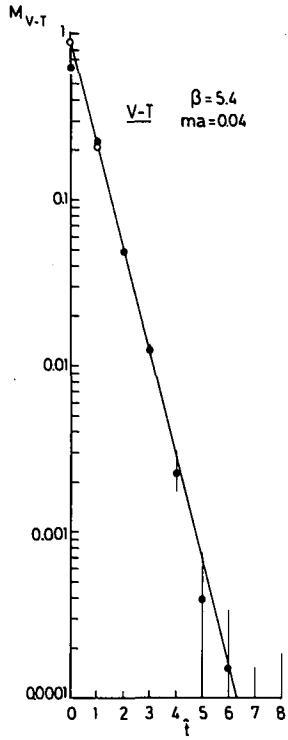

Fig. 3. The correlation function M_{V-T} for $\beta = 5.4$ and $ma = 0.04$. The solid circles are the results of our calculation. The open circles result from subtracting the fitted (oscillating) B contribution from M_{V-T}. When no open circles are drawn they coincide with the solid circles. The solid line is the fit as described in the text.

values of β for determining m_B. At $\beta = 5.9$ and $\hat{t} \geqslant 7 M_{V-T}$ tends to depart from the exponential decay and flatten off. The effect is most dramatic for the smaller quark masses (cf. figs. 11a, b) and goes away for $ma \geqslant 0.08$. Smaller quark masses mean that the quark paths will spread over a larger volume of the lattice, and the larger $\hat{t}$ is the larger will be the volume be, until eventually they will feel the boundary. The spatial extent of the lattice (in physical units) at $\beta = 5.9$ is about 30% smaller than at $\beta = 5.7$. This leads us to interpret the flattening off as a finite size effect. M_s (figs. 4, 8, 12a, b) also oscillates, but with decreasing tendency as β increases. All mesonic correlation functions show an increasing admixture of higher excited states (i.e. departure from a single exponential) with increasing β which means that one must go to larger $\hat{t}$ (and eventually to larger spatial lattices in order not to run into conflict with finite size effects) to obtain the ground state mass. The baryonic correlation function B (figs. 5, 9, 13a, b) oscillates in a most striking manner. To elucidate its behaviour we call attention to eq. (24), according to which the nucleon contributes with equal sign to even and odd $\hat{t}$ while the N′ and N^- contribute with opposite relative sign to even $\hat{t}$and with equal relative sign to odd $\hat{t}$ (the overall

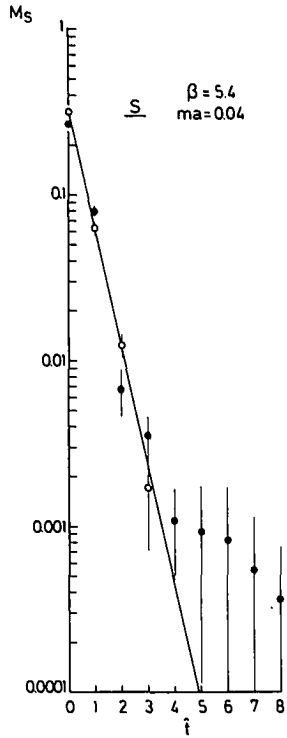

Fig. 4. The correlation function M_S for $\beta = 5.4$ and $ma = 0.04$. The solid circles are the results of our calculation. The open circles result from subtracting the fitted (oscillating) "pion" contribution from M_S. When no open circles are drawn they coincide with the solid circles. The solid line is the fit as described in the text.

signs in (21) and (24) have been chosen such that K_N, $K_{N'}$, K_{N^-} are positive). It appears that N′ and N⁻ and their recurrences cancel nearly completely at even $\hat{t}$ which means that $m_{N'} \approx m_{N^-}$, $K_{N'} \approx K_{N^-}$, etc. This is not surprising. A straightforward analysis of the quark propagator yields in the limit of zero quark mass:

$$B_+(t) + B_-(t) = O(\langle\bar{\psi}\psi\rangle^3[e^{-m_N 2t} - e^{-m_N(T-2t)}]) \xrightarrow[a\to 0]{} 0\,,$$

$$B_+(t) - B_-(t) = O(\text{const}\,[e^{-m_N 2t} + e^{-m_N(T-2t)}])\,, \tag{27}$$

which only leaves two possibilities: $K_N = O(\langle\bar{\psi}\psi\rangle^3)$, $m_{N'} \approx m_{N^-}$, $K_{N'} \approx K_{N^-}$ and $m_N \approx m_{N^-}$, $m_{N'} \approx m_{N'^-}$, $K_N - K_{N^-} = O(\langle\bar{\psi}\psi\rangle^3)$, $K_{N'} - K_{N'^-} = O(\langle\bar{\psi}\psi\rangle^3)$ (where N'^- denotes the first excited $\frac{1}{2}^-$ state).

3.3. EXTRACTION OF HADRON MASSES

To obtain the hadron mass spectrum, we fit our calculated mesonic and baryonic correlation functions by a few masses as we will describe now.

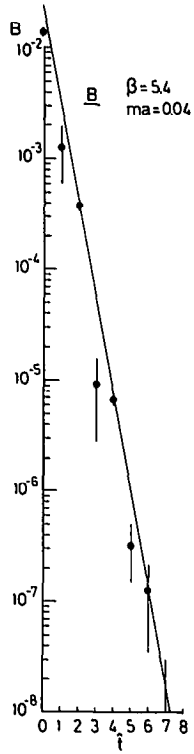

Fig. 5. The correlation functions B for $\beta = 5.4$ and $ma = 0.04$. The solid circles are the results of our calculations. The solid line is the fit described in the text.

M_{PS}: we fit M_{PS} by two masses, m_π and $m_{\pi'}$. The result is shown for a few of the correlation functions by the curves in figs. 2, 6, 10a, b.

M_{V-T}: we fit M_{V-T} by two masses, m_ρ and m_B, at $\beta = 5.4$ and by three masses, m_ρ, $m_{\rho'}$ and m_B, at $\beta = 5.7$ and $\beta = 5.9$. To demonstrate the quality of our fits we subtract the resulting B contribution from M_{V-T}. This gives the open circles in figs. 3, 7, 11a, b. When no open circles are drawn they coincide with the solid circles, that means the B contribution has died off. The curves in the figures are our fits for $K_B = 0$ which should interpolate the open circles. In ref. [1] we have, at $\beta = 5.7$, fitted the $2 \leq \hat{t}$ tail of M_{V-T} by m_ρ and m_B which gives the same result for m_ρ.

M_{PV}: we fit M_{PV} by m_{A_1} and m_ρ at $\beta = 5.4$ and by m_{A_1}, m_ρ and $m_{\rho'}$ at $\beta = 5.7$ and $\beta = 5.9$. We take m_ρ and $m_{\rho'}$ from our fit of M_{V-T}.

M_S: there is only a noticeable oscillation of M_S at $\beta = 5.4$. At this β we fit M_S by two masses, m_ε and m_π. We do not fix m_π at the value obtained from M_{PS}. It appears that a much larger "m_π" is needed here to describe M_S. As in case of M_{V-T} we subtract the resulting "π" contribution from M_S (when visible) which gives the open circles in fig. 4. The curve in that figure is our fit for $K'_\pi = 0$. At $\beta = 5.7$ we fit M_S by a single mass, m_ϵ. The result is the curve in fig. 8. In ref. [1] we have fitted

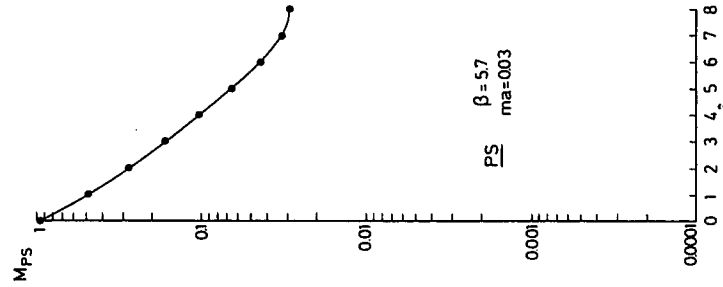

Fig. 6. Same as fig. 2 but for $\beta = 5.7$ and $ma = 0.03$.

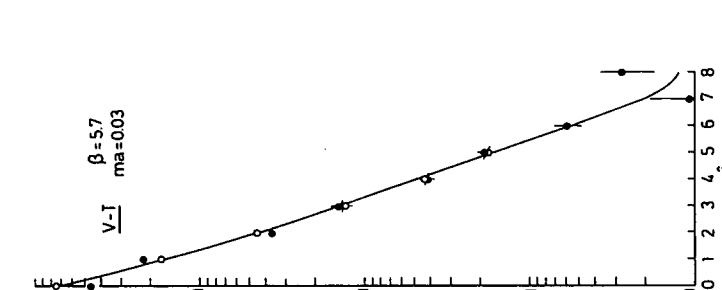

Fig. 7. Same as fig. 3 but for $\beta = 5.7$ and $ma = 0.03$.

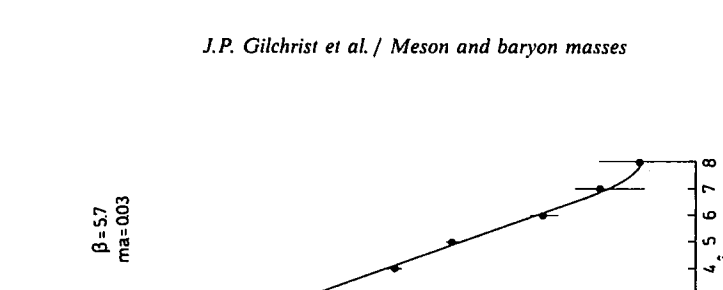

Fig. 8. Same as fig. 4 but for $\beta = 5.7$ and $ma = 0.03$. Because of the small oscillations the "pion" subtracted correlation function is not shown separately.

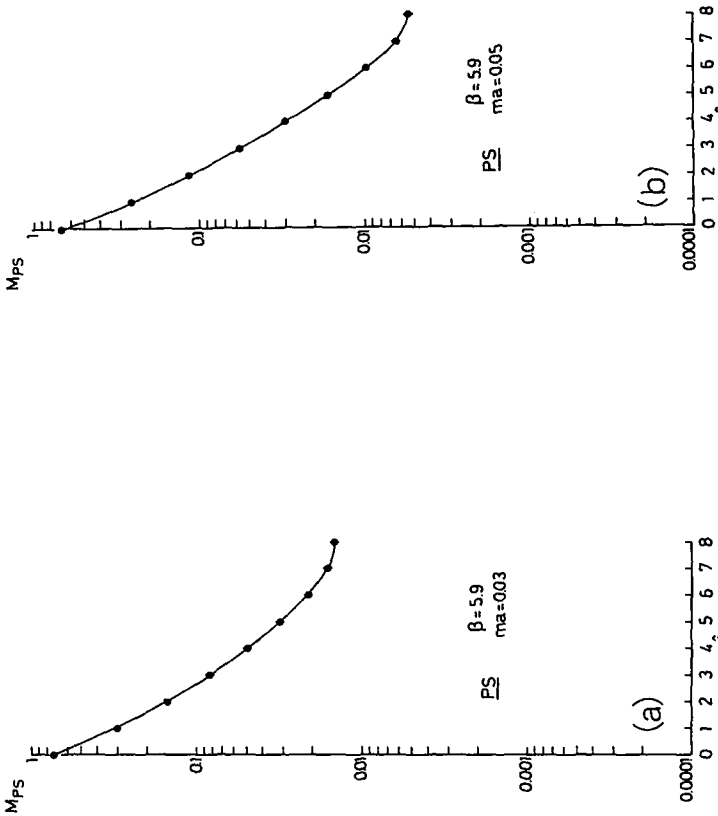

Fig. 10. Same as fig. 2 but for $\beta = 5.9$ and (a) $ma = 0.03$, and (b) $ma = 0.05$.

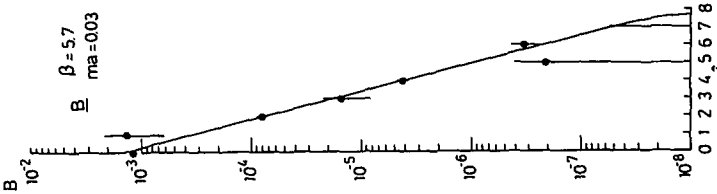

Fig. 9. Same as fig. 5 but for $\beta = 5.7$ and $ma = 0.03$.

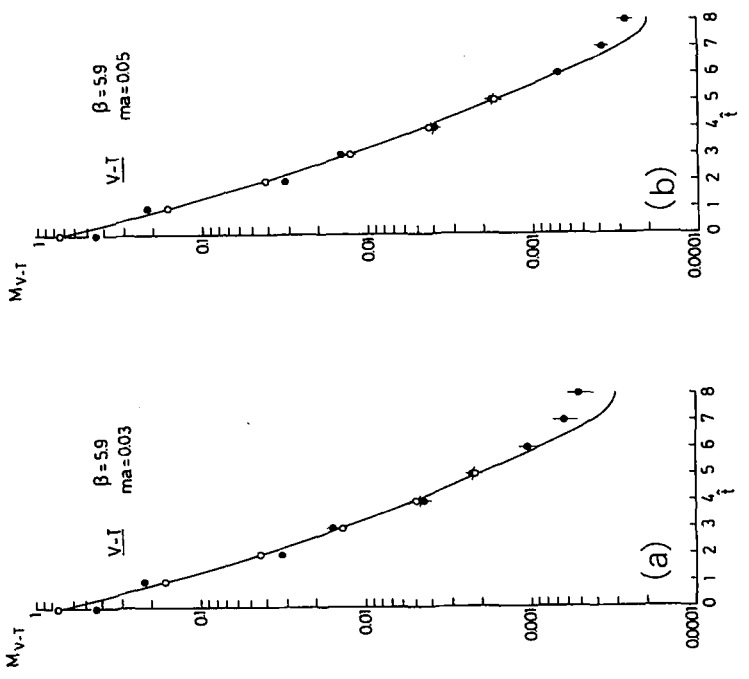

Fig. 11. Same as fig. 3 but for $\beta = 5.9$ and (a) $ma = 0.03$, and (b) $ma = 0.05$.

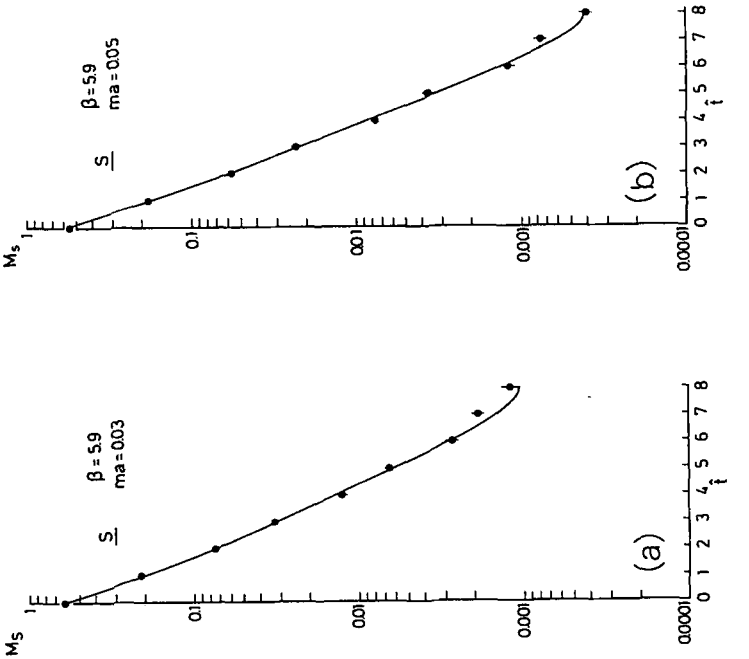

Fig. 12. Same as fig. 8 but for $\beta = 5.9$ and (a) $ma = 0.03$, and (b) $ma = 0.05$.

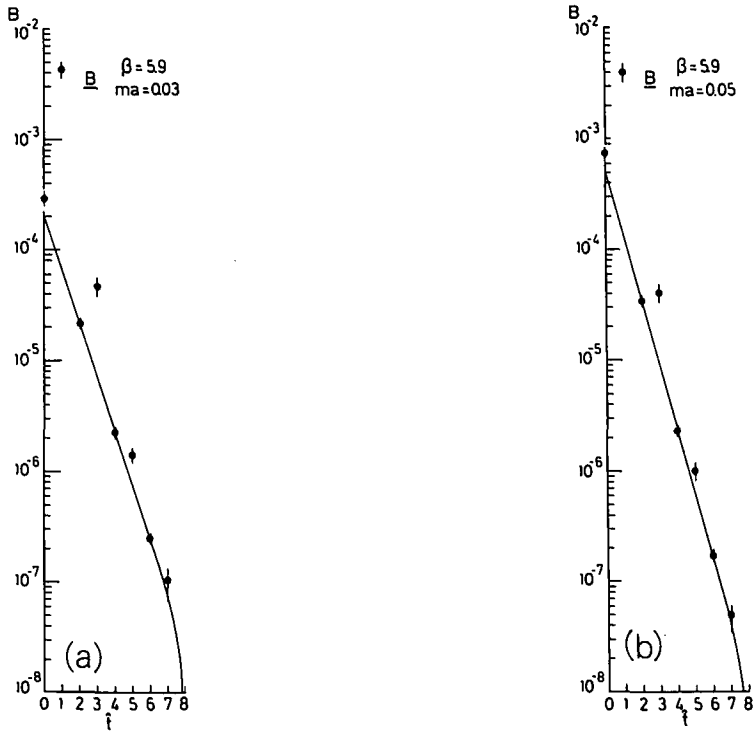

Fig. 13. Same as fig. 5 but for $\beta = 5.9$ and (a) $ma = 0.03$, and (b) $ma = 0.05$.

the $2 \leq \hat{t}$ tail of M_S by m_ε and m_π which gives the same value of m_ε and indicates how stable the fits are. At $\beta = 5.9$ it is no longer possible to describe M_S by a single scalar meson. We fit M_S by m_ε and $m_{\varepsilon'}$ which results in the curves in figs. 12a, b.

B: at even $\hat{t}$ the baryonic correlation function B falls, except for $\hat{t} = 0$, very nicely on a single exponential curve (to be precise: $e^{-m_N 2t} - e^{-m_N(T-2t)}$) as shown in figs. 5, 9, 13a, b. This led us to conclude earlier on that the N′ and N⁻ contributions cancel at even times. The slope of the curve gives us m_N. At odd $\hat{t}$ we fit B by $m_{N'} = m_{N^-}$ in addition to the nucleon contribution.

4. Meson and baryon masses

We shall now discuss the results of the calculation. We begin with the pion and the determination of the quark mass.

4.1. THE PION AND QUARK MASS

The results for m_π are shown in figs. 14–16 for all our calculations, that is for three values of β and three quark masses each. We find that m_π^2 vanishes linearly

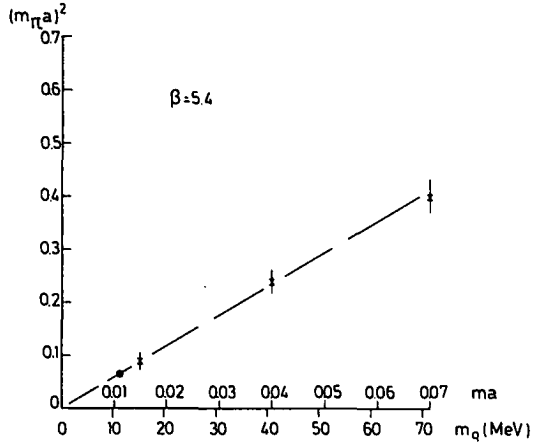

Fig. 14. $(m_\pi a)^2$ as a function of ma (m_q) for $\beta = 5.4$. The solid circle on the linear extrapolation curve marks the position of the physical pion using (29), (30).

with the quark mass, i.e. $m_\pi^2 \sim m$, which is what one expects for a Goldstone pion. The dashed lines in the figures are parameterized by

$$\beta = 5.4\,, \quad (m_\pi a)^2 = 5.86\, ma\,,$$
$$\beta = 5.7\,, \quad (m_\pi a)^2 = 7.60\, ma\,,$$
$$\beta = 5.9\,, \quad (m_\pi a)^2 = 6.86\, ma\,. \tag{28}$$

We obtain the quark mass by inserting the physical pion mass into the mass relations (28). For the lattice spacing a we assume the two-loop formula

$$a(\beta) = \frac{83.5}{\Lambda_{\text{mom}}}\, e^{-(4\pi^2/33)\beta}\left(\tfrac{8}{33}\pi^2\beta\right)^{51/121}. \tag{29}$$

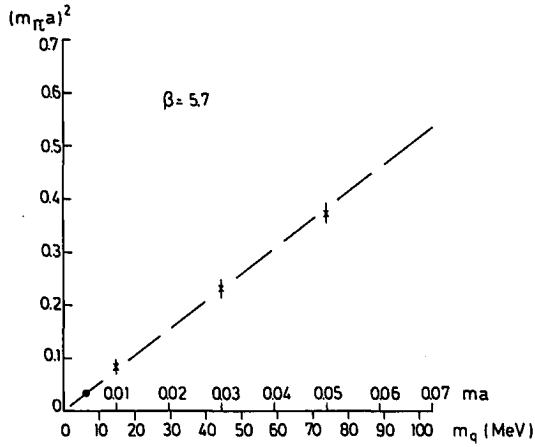

Fig. 15. Same as fig. 14 but for $\beta = 5.7$.

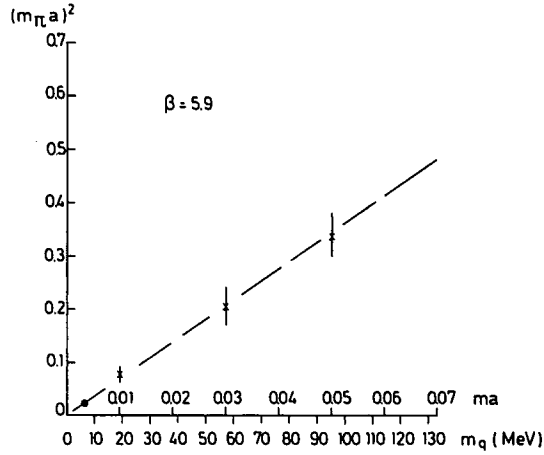

Fig. 16. Same as fig. 14 but for $\beta = 5.9$.

We depart from ref. [1] in determining the scale parameter. In this work we fit Λ_{mom} to give the right rho mass at $\beta = 5.7$. We obtain (cf. later on)

$$\Lambda_{\text{mom}} = 210 \text{ MeV}, \tag{30}$$

which we shall use throughout the present paper. (This is only slightly different from the previously used value of $\Lambda_{\text{mom}} = 200$ MeV.) The quark mass that is of interest to us here is the renormalization group invariant quark mass, m_q, which is given by

$$m_q = \alpha_{\text{mom}}^{-4/11} m,$$

$$\alpha_{\text{mom}} = \frac{4\pi}{11 \ln(\pi/a\Lambda_{\text{mom}})^2 + \frac{102}{11} \ln\ln(\pi/a\Lambda_{\text{mom}})^2} \approx \frac{3}{2\pi(\beta - 2.742)}. \tag{31}$$

The quantitative connexion of the bare quark mass ma with m_q is shown on the horizontal lines in figs. 14–16. For m_q we find

$$\beta = 5.4, \quad m_q = 11.5 \text{ MeV},$$

$$\beta = 5.7, \quad m_q = 6.5 \text{ MeV},$$

$$\beta = 5.9, \quad m_q = 6.3 \text{ MeV}. \tag{32}$$

The solid circles in figs. 14–16 indicate the position of the physical pion mass on the curves (28).

We observe that the renormalization group invariant quark mass scales for $\beta \geqslant 5.7$ and that the mass value of ≈ 6.5 MeV is in agreement with current algebra estimates (for a review see [13]). At $\beta = 5.4$ the quark mass comes out to be a factor of ≈ 2 larger than that at $\beta = 5.7$ and $\beta = 5.9$. The reason is that $\beta = 5.4$ is for the pion already in the strong coupling region as we will see in more detail later on.

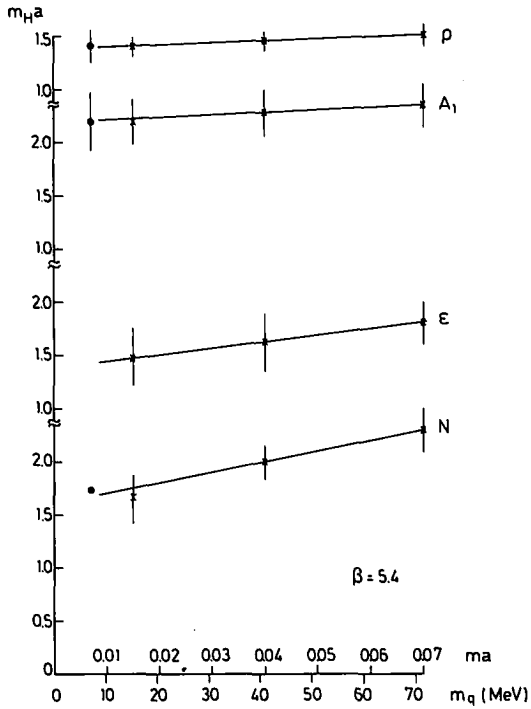

Fig. 17. The hadron masses, $m_H a$ as a function of ma (m_q) for $\beta = 5.4$. The solid circles at the physical quark mass, $m_q = 6.5$ MeV, indicate their experimental values using (29), (30).

4.2. THE LOW-LYING HADRON SPECTRUM

The results for m_ρ, m_{A_1}, m_ε and the nucleon mass m_N are shown in figs. 17–19. The solid circles at the previously obtained scaling quark mass $m_q = 6.5$ MeV, denote their experimental values. It should be noted that in our calculation of the mass of the iso-singlet scalar state, m_ε, we have only taken the connected part (via a $q\bar{q}$ pair) of the correlation function into account (cf. eq. (14)).

We may fit the dependence of m_ρ, m_{A_1}, m_ε and m_N on the quark mass by a straight line. The result is

$$\begin{aligned}
\beta = 5.4, \quad m_\rho a &= 1.38 + 1.71\, ma\,, \\
m_{A_1} a &= 2.20 + 2.14\, ma\,, \\
m_\varepsilon a &= 1.38 + 6.14\, ma\,, \\
m_N a &= 1.60 + 10.00\, ma\,, \\
\beta = 5.7, \quad m_\rho a &= 0.98 + 4.10\, ma\,, \\
m_{A_1} a &= 1.61 + 3.30\, ma\,,
\end{aligned} \tag{33}$$

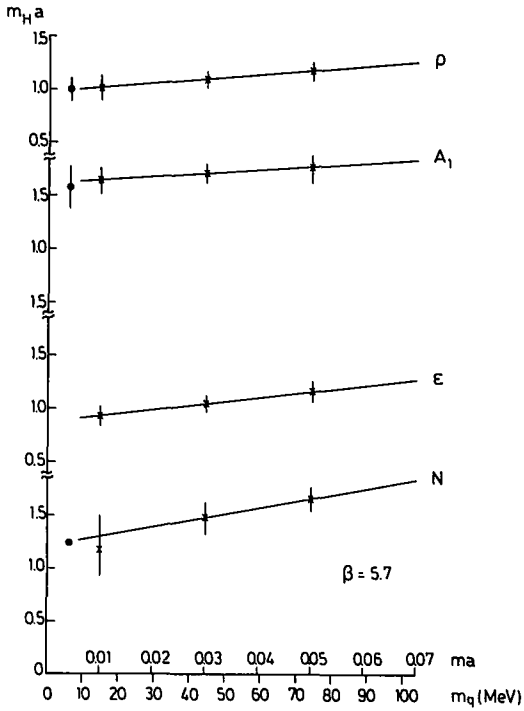

Fig. 18. Same as fig. 17 but for $\beta = 5.7$.

$$m_\varepsilon a = 0.88 + 5.70\, ma\,,$$
$$m_N a = 1.21 + 9.00\, ma\,, \tag{34}$$
$$\beta = 5.9, \quad m_\rho a = 0.75 + 3.57\, ma\,,$$
$$m_{A_1} a = 1.37 + 3.29\, ma\,,$$
$$m_\varepsilon a = 0.63 + 5.71\, ma\,,$$
$$m_N a = 0.88 + 8.29\, ma\,, \tag{35}$$

which correspond to the solid lines in figs. 17–19. Note that the dependence of the hadron masses (33)–(35) on the quark mass is rather weak over the range of quark masses we consider. We shall use the above linear mass fits to extrapolate the hadron masses to the physical quark mass of $m_q = 6.5$ MeV. We obtain in MeV units ($\Lambda_{mom} = 210$ MeV)

$$\beta = 5.4\,, \quad m_\rho = (750 \pm 40)\ \text{MeV}\,,$$
$$m_{A_1} = (1200 \pm 110)\ \text{MeV}\,,$$
$$m_\varepsilon = (770 \pm 110)\ \text{MeV}\,,$$
$$m_N = (915 \pm 80)\ \text{MeV}\,, \tag{36}$$

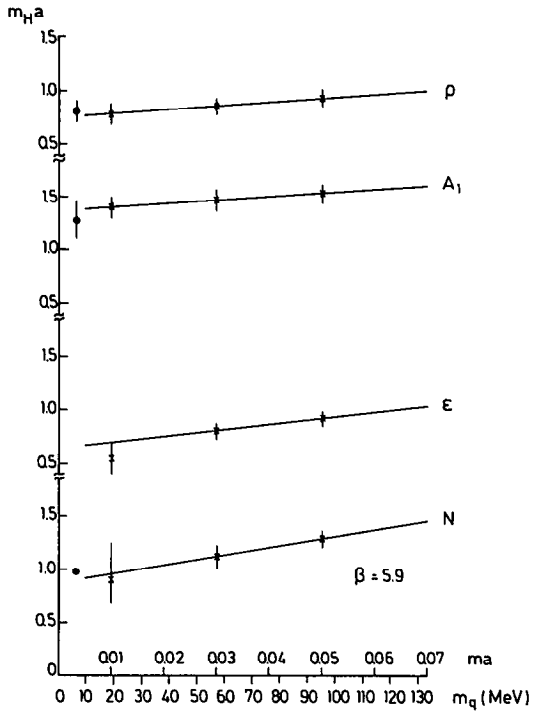

Fig. 19. Same as fig 17 but for $\beta = 5.9$.

$$\begin{aligned}
\beta = 5.7\,, \quad m_\rho &= (770 \pm 90)\ \text{MeV}\,, \\
m_{A_1} &= (1250 \pm 90)\ \text{MeV}\,, \\
m_\varepsilon &= (690 \pm 50)\ \text{MeV}\,, \\
m_N &= (960 \pm 100)\ \text{MeV}\,, \qquad (37) \\
\beta = 5.9\,, \quad m_\rho &= (730 \pm 90)\ \text{MeV}\,, \\
m_{A_1} &= (1310 \pm 100)\ \text{MeV}\,, \\
m_\varepsilon &= (630 \pm 100)\ \text{MeV}\,, \\
m_N &= (860 \pm 120)\ \text{MeV}\,. \qquad (38)
\end{aligned}$$

We find the mass to be stable against the fitting procedure. If at $\beta = 5.7$ we fit the $2 < \hat{t} < 14$ tail of M_{V-T} by the ρ (and B) mass only, we obtain exactly the same value [1]. That this is a viable procedure can be seen from fig. 7 in which the open circles fall (for $\hat{t} > 2$) on a single exponential. This also tells us that the rho mass quoted is not biased by contamination with excited states. At $\beta = 5.9$ we also reproduce the quoted rho mass (within errors) if we fit the $3 < \hat{t} < 13$ tail of M_{V-T} by the ρ (and B) mass only.

The hadron masses (36)–(38) are consistent with asymptotic scaling. Moreover, within the statistical errors m_ρ, m_{A_1} and m_N agree with experiment. We find this quire remarkable, in particular as Λ_{mom} is not really a free parameter. As we shall see later on various other physical quantities also calculated on the lattice [9] narrow it down to $\Lambda_{mom} \approx 200$ MeV. The ε meson will mix with the 0^{++} glueball state. But since m_ε and the 0^{++} glueball mass [14] are almost identical this will perhaps not shift either of the masses significantly. The proximity of m_ε and the 0^{++} glueball mass might explain why the deconfining phase transition and chiral symmetry restoration occur at the same temperature [15].

We are not in a position yet to quote any reliable numbers for the B meson mass.

4.3. RENORMALIZATION GROUP SCALING

In QCD any value of the quark mass is conceivable. The more general statement of renormalization group scaling therefore is that the calculated hadron masses, when expressed in terms of a fixed scale via the continuum renormalization group eq. (29) for $a(\beta)$ and in terms of a fixed, but arbitrary, renormalization group invariant quark mass (30), should not depend on β. Accordingly we plot in fig. 20

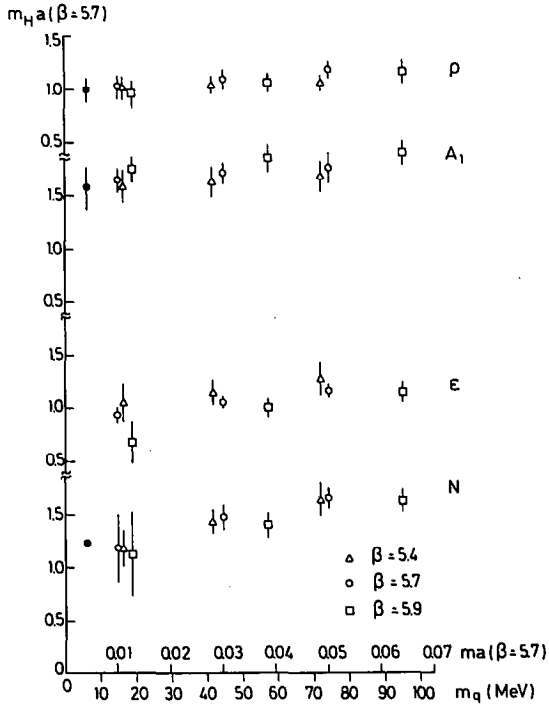

Fig. 20. The hadron masses m_H in units of a^{-1} ($\beta = 5.7$) as a function of the renormalization group invariant quark mass m_q ($ma(\beta = 5.7)$) combined for $\beta = 5.4$, $\beta = 5.7$ and $\beta = 5.9$.

the hadron masses obtained at the three different values of β in the dimensionless product form $m_H a(\beta = 5.7)$ versus the renormalization group invariant quark mass. We obtain $m_H a(\beta = 5.7)$ from $m_H a(\beta)$ by the use of the two-loop formula (29).

We find that within the statistical errors m_ρ, m_{A_1}, m_ε and m_N scale more or less, for all invariant quark masses considered in this work. For the rho mass, which has the smallest errors, the agreement with the desired continuum renormalization group behaviour is quite remarkable. In case of the nucleon, on the other hand, the errors could hide a O(10%) systematic deviation. But this would not surprise us since at $\beta = 5.9$ the 10^3 lattice is only ≈ 2 fm across, which is less than twice the (supposed) nucleon diameter, so that finite size effects might show up here.

4.4. f_π

Using the current algebra relation

$$f_\pi^2 m_\pi^2 = 4 m_q \langle \bar{\psi}\psi \rangle_{\text{inv}} , \tag{39}$$

and the previously calculated [3] $\langle \bar{\psi}\psi \rangle_{\text{inv}}$ as input, we can calculate f_π from the slopes given in eq. (28). We obtain

	input [3]: $\langle \bar{\psi}\psi \rangle_{\text{inv}}^{1/3}$	f_π
$\beta = 5.4$	270 MeV	210 MeV
$\beta = 5.7$	245 MeV	140 MeV
$\beta = 5.9$	230 MeV	120 MeV

(40)

(remember that we have changed Λ_{mom} from 200 to 210 MeV). This is to be compared to the experimental value [13] of $f_\pi = (131.9 \pm 0.1)$ MeV. That f_π does not scale at $\beta = 5.4$ is (again) due to the fact that $\beta = 5.4$ is for the pion already in the strong coupling region (see later on).

4.5. RECURRENCES

The results for $m_{\pi'}$ and $m_{\rho'}$ are summarized in fig. 21 (in the same kind of plot as in fig. 20). Within the errors $m_{\pi'}$ scales for $\beta \geqslant 5.7$, while at $\beta = 5.4$ $m_{\pi'}$ falls much below the "scaling" value. For $m_{\rho'}$ we have only results for $\beta \geqslant 5.7$ (since at $\beta = 5.4$ we fit the correlation functions by m_ρ and m_B only). Within the errors $m_{\rho'}$ scales also. In physical units ($a^{-1}(\beta = 5.7) = 0.77$ GeV) we obtain

$$m_{\pi'} = (1100 \pm 150) \text{ MeV} ,$$

$$m_{\rho'} = (1600 \pm 200) \text{ MeV} . \tag{41}$$

For the baryon masses $m_{N'}$ and m_{N^-} we obtain useful numbers only at $\beta = 5.9$ (cf. figs. 5, 9, 13a, b). But the errors are still too large to quote a value, in particular as

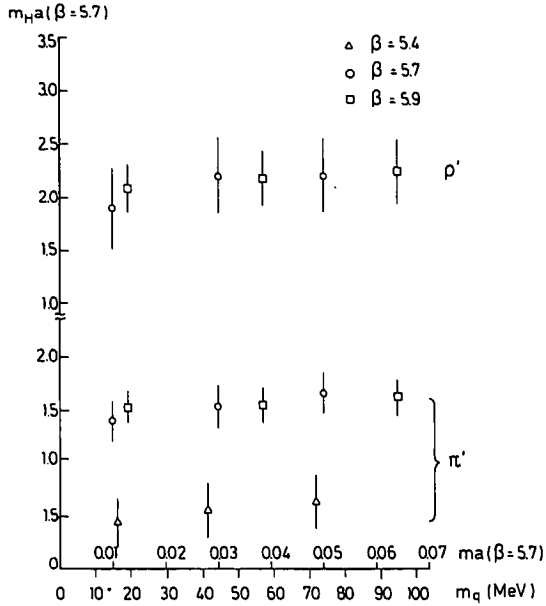

Fig. 21. Same as fig. 20 but for $m_{\pi'}$ and $m_{\rho'}$.

there is a strong admixture of higher states at odd $\hat{t}$. It is interesting to note that the rate of admixture of excited states does not depend significantly on the quark mass.

4.6. COMPARISON WITH STRONG COUPLING CALCULATION

The low-lying meson and baryon masses for Kogut–Susskind quarks have also been calculated in the strong coupling limit [16]. To answer the question of how far we are in the continuum region and to make the point that Monte Carlo techniques are indispensable for obtaining the correct continuum masses, even the mass ratios, we compare our results with the strong coupling calculations [16] in figs. 22 to 26. We (finally) see that for the pion (fig. 22) the continuum region begins only at $\beta \gtrsim 5.5$ while for the rest of the masses $\beta = 5.4$ seems to be already well in the continuum region. The transition from the strong coupling to the scaling region is by no means smooth for the pion and the A_1 meson, what perhaps signals the presence of nearby singularities in the complex β plane. It is inconceivable that the strong coupling expansions will be able to reproduce this behaviour. Hence we are not surprised that the strong coupling calculations fail to describe the pion and the mass of the A_1 meson, while m_ρ and m_N (which extrapolate smoothly) can be fitted.

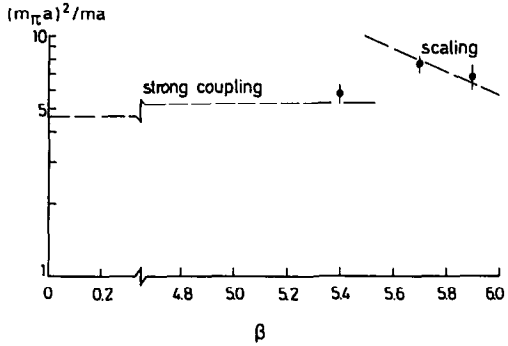

Fig. 22. $(m_\pi a)^2/ma$ as a function of β. The solid circles are the results of our calculation. The horizontal dashed line is the result of the strong coupling calculation in ref. [16].

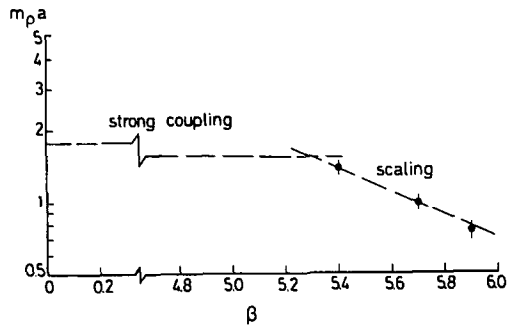

Fig. 23. $m_\rho a$ as a function of β. The solid circles are the results of our calculation. The horizontal dashed line is the result of the strong coupling calculation in ref. [16].

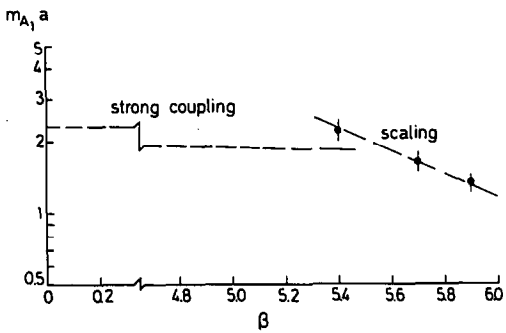

Fig. 24. Same as fig. 23 but for $m_{A_1} a$.

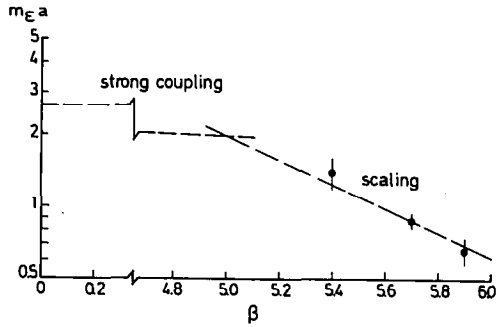

Fig. 25. Same as fig. 23 but for $m_\varepsilon a$.

5. Conclusions

In the present work we have calculated the lowest-lying meson and baryon masses at three values of β using the Kogut–Susskind discretization of the fermion action. We differ from previous spectrum calculations by computing the masses directly at the small quark masses of phenomenological interest. This eliminates the ambiguities associated with large extrapolations in the quark mass over hundreds of MeV. (Other authors calculate typically at $m_q \gtrsim 200$ MeV.)

We have shown that the hadron masses we have calculated, including the quark mass, adhere to a statistically significant extent to the renormalization group behaviour, implying that they are representative of continuum QCD. This, and the overall agreement with experiment, is encouraging and more than we could expect on these rather coarse lattices and from working at the "edge" of the continuum region.

To go further into the continuum we have to go to larger lattices. We feel that $\beta = 5.9$ is as far we we can go on the 10^3 lattice. Even here we begin already to observe finite size effects. To consolidate our results we are presently repeating the calculation on a 16^4 lattice.

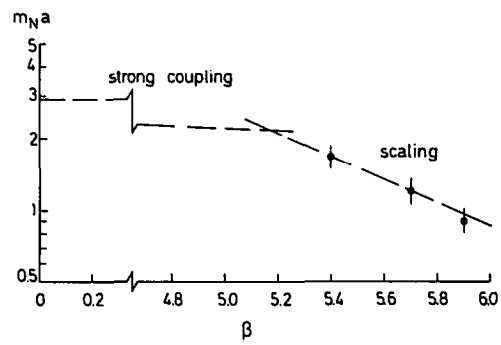

Fig. 26. Same as fig. 23 but for $m_N a$.

The scale parameter Λ_{mom} is known from several other physical quantities with varying accuracy. In the following table we have compiled some recent values

$\Lambda_{\text{mom}}(\beta \approx 5.7)$	*from*	*input*
210 ± 30 MeV	rho mass (this work)	m_ρ
195 ± 25 MeV	chiral condensate [3]	$\langle \bar{\psi}\psi \rangle_{\text{rrev}}^{1/3} = 225 \pm 25$ Mev [3]
180 ± 20 MeV	gluon condensate [17, 9]*	$\left\langle \frac{\alpha_s}{\pi} F_{\mu\nu} F_{\mu\nu} \right\rangle = 336 \pm 10$ MeV [18]
230 ± 30 MeV	string tension [19]**	$\sqrt{K} = 400$ MeV
200 ± 35 MeV	2^{++} glueball mass [20]	$m_\theta = 1670 \pm 50$ MeV(?) [21] (42)

which centre around $\Lambda_{\text{mom}} \approx 200$ MeV (one should be aware though that the string tension seems not to scale). Thus we may say that we begin to obtain a consistent picture of quark and gluon physics in quenched QCD. Wilson fermions, on the other hand, give a value of Λ_{mom} which is about twice as large.

The numerical calculations have been done on the Siemens 7.882 at the University of Hamburg and on the Cyber 205 at the University of Karlsruhe. We are grateful for the generous facilities provided by the computer centre of the University of Hamburg and for the support of the DESY directorate in purchasing time on the Cyber 205. We are indebted to Drs. D. Ponting and I. Duff for useful discussions and to Dr. Schäfer from CDC for computational assistence. H.S. and M.T. thank Prof. F. Gutbrod for the hospitality of the DESY Theory Group during part of this work, and J.P.G. thanks the SERC and the Royal Society for a fellowship.

Note added

We are aware that (continuum) parity is not an invariance of the classical lattice action. However we have reason to believe that it has already been largely restored (dynamically) at the present values of β: for example, we find flavour mixing in $\langle \bar{\psi}\psi \rangle$ to be very small. This has led us to parametrize the correlation functions in the form (15) and (21). Such details of the parametrization make only a small difference at large $\hat{t}$, and in fact these differences would be masked by our present statistical and systematic errors. We will address this question in more detail when we have accumulated higher statistics.

As far as the question of scaling is concerned we would like to add that the recently calculated ρ mass of Billoire, Marinari and Petronzio (preprint CERN-TH-3838) at $\beta = 6.0$ is in good agreement with our values, and renormalisation group scaling, if we use a *linear* extrapolation in quark mass on their data. Testing scaling

* The second reference in [17] gives an earlier calculation which is consistent with ours.

** Ref. [19] gives recent calculations on large lattices.

(as we have done in this paper) is of crucial importance, because the accessible range of lattice spacings is such that one might well expect some quantities not to have yet reached their continuum limits. Indeed while the 0^{++} and 2^{++} glueball masses [14] and the chiral condensate, $\langle\bar{\psi}\psi\rangle$ [3] show, at most, small violations of scaling, this appears not to be the case for the string tension [6] or the deconfining temperature (for a recent paper, and references, see Karsch and Petronzio, preprint CERN-TH-3797).

References

[1] J.P. Gilchrist, G. Schierholz, H. Schneider and M. Teper, Phys. Lett. 136B (1984) 87

[2] J. Kogut and L. Susskind, Phys. Rev. D11 (1975) 395;
L. Susskind, Phys. Rev. D16 (1977) 303;
T. Banks, J. Kogut and L. Susskind, Phys. Rev. D13 (1976) 1043;
T. Banks, S. Raby, L. Susskind, J. Kogut, D.R.T. Jones, P.H. Scharbach and D. Sinclair, Phys. Rev. D15 (1976) 1111;
H.S. Sharatchandra, H.J. Thun and P. Weisz, Nucl. Phys. B192 (1981) 205

[3] I.M. Barbour, P. Gibbs, J.P. Gilchrist, G. Schierholz, H. Schneider and M. Teper, Phys. Lett. 136B (1984) 80

[4] K.G. Wilson, Erice lectures (1975)

[5] M. Fukugita, T. Kaneko and A. Ukawa, Phys. Lett. 130B (1983) 199

[6] H. Lipps, G. Martinelli, R. Petronzio and F. Rapuano: CERN preprint TH-3548 (1983);
P. Hasenfratz, I. Montvay, DESY preprint 83-072 (1983)

[7] H. Hamber and G. Parisi, Phys. Rev. Lett. 47 (1981) 1792;
E. Marinari, G. Parisi and C. Rebbi, Phys. Rev. Lett. 47 (1981) 1795;
D. Weingarten, Phys. Lett. 109B (1982) 57;
A. Hasenfratz, P. Hasenfratz, Z. Kunzt and C.B. Lang, Phys. lett. 110B (1982) 289; 117B (1982) 81;
H. Hamber and G. Parisi, Phys. Rev. D27 (1983) 208;
F. Fucito, G. Martinelli, C. Omero, G. Parisi, R. Petronzio and F. Rapuano, Nucl. Phys. B210 (1982) 407;
D. Weingarten, Nucl. Phys. B215 (1983) 1;
K.C. Bowler, E. Marinari, G.S. Pawley, F. Rapuano and D.J. Wallace, Nucl. Phys. B220 (1983) 137;
R. Gupta and A. Patel, Nucl. Phys. B226 (1983) 152;
C. Bernard, T. Draper, K. Olynyk and M. Rushton, Nucl. Phys. B220 (1983) 508

[8] H. Lipps, G. Martinelli, R. Petronzio and F. Rapuano, CERN preprint TH-3548 (1983);
P. Hasenfratz and I. Montvay, DESY preprint 83-072 (1983);
K.C. Bowler, G.S. Pawley and D.J. Wallace, Edinburgh preprint 83/262 (1983)

[9] M. Tepers LAPP preprint TH-91 (1983)

[10] K.C. Bowler and D.J. Wallace, private communication

[11] H. Kluberg-Stern, A. Morel, O. Napoly and B. Petersson, Nucl. Phys. B220 [FS8] (1983) 447;
J. Kogut, M. Stone, H. Wyld, S. Shenker, J. Shigemitsu and D. Sinclair, Nucl. Phys. B225 [FS9] (1983) 326

[12] H. Hamber and G. Parisi, Phys. Rev. D27 (1983) 208

[13] J. Gasser and H. Leutwyler, Phys. Reports 87C (1982) 78

[14] K. Ishikawa, A. Sato, G. Schierholz and M. Teper, Z. Phys. C21 (1983) 167;
C. Michael and I. Teasdale, Nucl. Phys. B215 (1983) 433;
B. Berg and A. Billoire, Nucl. Phys. B221 (1983) 109;
G. Schierholz and M. Teper, Phys. Lett. 136B (1984) 64;
A. König, K.H. Mütter, J. Paech and K. Schilling, Wuppertal preprint 83-26 (1983)

[15] J. Kogut, M. Stone, H.W. Wyld, W.R. Gibbs, J. Shigemitsu, S.H. Shenker and D.K. Sinclair, Illinois preprint ILL-(TH)-82-39 (1982)

[16] T. Jolicoeur, H. Kluberg-Stern, M. Lev, A. Morel and B. Petersson, Saclay preprint SPhT/83/70; Nucl. Phys. B235 [FS11] (1934) 455
[17] G. Schierholz and M. Tepers, in preparation;
E.M. Ilgenfritz and M. Müller-Preussker, Phys. Lett. 119B (1982) 395
[18] G. Launer, S. Narison and R. Tarrach, CERN preprint TH-3712 (1983)
[19] M. Fukugita, T. Kaneko and A. Ukawa, KEK preprint TH 63 (1983);
F. Gutbrod, P. Hasenfratz, I. Montvay and Z. Kunszt, CERN preprint TH-3591 (1983)
[20] K. Ishikawa, A. Sato, G. Schierholz and M. Teper, Z. Phys. C21 (1983) 167;
G. Schierholz and M. Teper, Phys. Lett. 136B (1984) 64
[21] E. Bloom, talk at the Paris Conf. (1982)